The Journal of Immunology

Absence of Vasoactive Intestinal Peptide Expression in Hematopoietic Cells Enhances Th1 Polarization and Antiviral Immunity in Mice

Jian-Ming Li, Lauren Southerland, Mohammad S. Hossain, Cynthia R. Giver, Ying Wang, Kasia Darlak, Wayne Harris, James Waschek and Edmund K. Waller

J Immunol 2011; 187:1057-1065; Prepublished online 15 June 2011;
doi: 10.4049/jimmunol.1100686
http://www.jimmunol.org/content/187/2/1057

The Journal of Immunology is published twice each month by
The American Association of Immunologists, Inc.,
1451 Rockville Pike, Suite 650, Rockville, MD 20852

Print ISSN: 0022-1767 Online ISSN: 1550-6606.

Absence of Vasoactive Intestinal Peptide Expression in Hematopoietic Cells Enhances Th1 Polarization and Antiviral Immunity in Mice

Jian-Ming Li,*[,1] Lauren Southerland,[†,1] Mohammad S. Hossain,* Cynthia R. Giver,* Ying Wang,* Kasia Darlak,* Wayne Harris,* James Waschek,[‡] and Edmund K. Waller*

Vasoactive intestinal peptide (VIP) induces regulatory dendritic cells (DC) in vitro that inhibit cellular immune responses. We tested the role of physiological levels of VIP on immune responses to murine CMV (mCMV) using VIP-knockout (VIP-KO) mice and radiation chimeras engrafted with syngenic VIP-KO hematopoietic cells. VIP-KO mice had less weight loss and better survival following mCMV infection compared with wild-type (WT) littermates. mCMV-infected VIP-KO mice had lower viral loads, faster clearance of virus, with increased numbers of IFN-γ^+ NK and NKT cells, and enhanced cytolytic activity of NK cells. Adaptive antiviral cellular immunity was increased in mCMV-infected VIP-KO mice compared with WT mice, with more Th1/Tc1-polarized T cells, fewer IL-10$^+$ T cells, and more mCMV-M45 epitope peptide MHC class I tetramer$^+$ CD8$^+$ T cells (tetramer$^+$ CD8 T cells). mCMV-immune VIP-KO mice had enhanced ability to clear mCMV peptide-pulsed target cells in vivo. Enhanced antiviral immunity was also seen in WT transplant recipients engrafted with VIP-KO hematopoietic cells, indicating that VIP synthesized by neuronal cells did not suppress immune responses. Following mCMV infection there was a marked upregulation of MHC-II and CD80 costimulatory molecule expression on DC from VIP-KO mice compared with DC from WT mice, whereas programmed death-1 and programmed death ligand-1 expression were upregulated in activated CD8$^+$ T cells and DC, respectively, in WT mice, but not in VIP-KO mice. Because the absence of VIP in immune cells increased innate and adaptive antiviral immunity by altering costimulatory and coinhibitory pathways, selective targeting of VIP signaling represents an attractive therapeutic target to enhance antiviral immunity. ***The Journal of Immunology*****, 2011, 187: 1057–1065.**

Vasoactive intestinal peptide (VIP) is a multifunctional endogenous polypeptide that modulates both innate and adaptive immunity at multiple levels of immune cell differentiation and activation (1). VIP is secreted by neurons (in both the central and peripheral nervous systems) (2) and by B cells, T cells, accessory cells, and other nonlymphoid cells (3–6). VIP and the closely related neuropeptide pituitary adenylyl cyclase-activating polypeptide (PACAP) bind to three known receptors: VPAC1, VPAC2, and PAC1. T cells and dendritic cells (DC) express VPAC1 and VPAC2, but not PAC1 (1). PAC1 is mainly expressed on neuron and endocrine cells in the brain and pituitary and adrenal glands, and selectively binds PACAP (7). Even though VIP and PACAP signal through the same receptors, PACAP does not fully compensate for the loss of VIP in VIP-knockout (VIP-KO) mice (8). VIP-KO mice lack compensatory increase in PACAP peptide expression, and expression of the VPAC1 and VPAC2 VIP receptors is diminished in brains of VIP-KO mice (8).

In adaptive immune responses, VIP polarizes CD4$^+$ T cells to an immunosuppressive Th2 response while suppressing the Th1 responses (9). T cell activation and differentiation induce VPAC2 expression, whereas VPAC1 is downregulated following stimulation of human blood T cells with anti-CD3 mAb plus PMA (10). VIP also acts on APC and regulates their function. Through the VPAC1 receptor, VIP leads to the development of bone marrow (BM)-derived tolerogenic DCs in vitro and in vivo (11). In a mouse model of allogeneic BM transplantation, DC that were differentiated in the presence of VIP, and then transplanted along with BM cells and splenic T cells, induced the generation of regulatory T cells and protected mice from acute graft versus host disease (12). Th2 polarization of immune responses by VIP-differentiated DC is most likely achieved through VIP downregulation of costimulatory signals on APC and inhibition of IL-1, TNF-α, IL-6, and IL-12 production (13). VIP suppresses the expression of the pattern recognition receptors TLR2 and TLR4 on APC (14, 15) and inhibits TLR3 signaling (16). Conversely, activation of APC through binding of ligands to TLR2, TLR4, and TLR7 downregulates VPAC2 expression (17).

Given the manifold effects of VIP on innate and adaptive immune responses, we explored the role of VIP in antiviral responses to CMV. Opportunistic CMV infection causes significant morbidity and transplant-related mortality in allogeneic BM transplantation

*Department of Hematology/Oncology, Winship Cancer Institute, Emory University, Atlanta, GA 30322; [†]Duke University School of Medicine, Duke University, Durham, NC 90586; and [‡]David Geffen School of Medicine, University of California, Los Angeles, Los Angeles, CA 90095

[1]J.-M.L. and L.S. contributed equally to this work.

Received for publication March 11, 2011. Accepted for publication May 13, 2011.

This work was supported by National Institutes of Health Grant R01 CA-74364-03 (to E.K.W.) and National Heart, Lung, and Blood Institute Grant P01Hl086773 (to J. Roback [principal investigator] and E.K.W.). J.-M.L. was supported by a research grant from the When Everyone Survives Foundation and the Emory University Research Council.

Address correspondence and reprint requests to Dr. Edmund K. Waller, 1365B Clifton Road NE, Room B5119, Winship Cancer Institute, Emory University Medical School, Atlanta, GA 30322. E-mail address: ewaller@emory.edu

The online version of this article contains supplemental material.

Abbreviations used in this article: BM, bone marrow; DC, dendritic cell; hCMV, human CMV; HSC, hematopoietic stem cell; KO, knockout; Lm-mCMV, *Listeria monocytogenes*-murine CMV; mCMV, murine CMV; PACAP, pituitary adenylyl cyclase-activating polypeptide; PD-1, programmed death-1; PD-L1, programmed death ligand-1; VIP, vasoactive intestinal peptide; WT, wild-type.

www.jimmunol.org/cgi/doi/10.4049/jimmunol.1100686

patients, and the pathogenesis of murine CMV (mCMV) infection in mice is similar to that in human CMV (hCMV) infection (18, 19). mCMV and hCMV exhibit 70% sequence similarity, comparable to the global level of DNA sequence homology between their natural hosts (20), and are predicted to contain ~170 and 165 open reading frames, respectively (21, 22). The large number of homogeneous open reading frames indicates that the two viruses are related, although immune evasive strategies of mCMV infection are quite different from those seen following hCMV infection (20), suggesting specific adaptation of a common ancestor virus to the immune environments of mice and humans (23). Furthermore, mice and humans have similar specific immune responses to their respective CMV (21, 24–26), with coordinated activities of innate and adaptive immune cells, including DC, macrophages, NK cells, T cells, and B cells (27–32). Whereas cellular and humoral immune response to mCMV is robust and effective in clearing the virus, mCMV infection also leads to immunosuppressive effects, including expression of m144, a MHC-I decoy that binds to NK cells and inhibits antiviral cytotoxicity (33, 34), and induction of a paralyzed DC phenotype, characterized by downregulation of MHC-I and MHC-II, costimulatory molecules, and proinflammatory cytokines (32). Hence, we were interested in whether interference with VIP signaling could enhance immune responses to mCMV infection. Previous studies have explored the effect of VIP on inflammation and allogeneic immunity using supraphysiological, pharmacological administration of purified VIP peptide agonist (3, 9). To study the immunomodulatory effects and antiviral immunity of physiological levels of VIP, we used VIP-KO mice (35) and VIP-KO hematopoietic chimeras (36). We hypothesized that mice lacking VIP expression would show an increased response to viral infection due to a lack of immunosuppressive counter-regulatory activity from DCs. We challenged VIP-KO mice and radiation chimeras engrafted with VIP-KO hematopoietic cells with two sources of mCMV Ag: a *Listeria monocytogenes* vaccine that expresses an immunodominant mCMV peptide (*Listeria monocytogenes*-mCMV [Lm-mCMV] vaccine) (37, 38) and an infectious strain of mCMV (37, 39). Our results demonstrate that VIP-KO mice and recipients engrafted with VIP-KO hematopoietic cells have augmented cellular immune responses to mCMV Ag, and improved survival after viral infection. The kinetics of Ag-specific primary and secondary immune responses were accelerated in VIP-KO mice and in mice reconstituted with VIP-KO hematopoietic cells, supporting the role of VIP in immune counter-regulatory pathways.

Materials and Methods

Mice

B6 strain (H-2K^b, CD45.2, CD90.2) VIP/peptide histidine isoleucine–KO mice have been previously described (35). Both male and female VIP-KO mice were used in experiments, using syngenic siblings as wild-type (WT) controls. Congenic strains of B6 mice were purchased from The Jackson Laboratory (Bar Harbor, ME) (H-2K^b, CD45.1, CD90.2) or were bred at the Emory University Animal Care Facility (Atlanta, GA) (H-2K^b, CD45.1/CD45.2). All mice were 8–10 wk old. Procedures conformed to the Guide for the Care and Use of Laboratory Animals, and were approved by the Emory University Institutional Animal Care and Use Committee. According to Institutional Animal Care and Use Committee guidelines, any mouse that lost ≥25% body weight was euthanized and recorded as dying on the following day for statistical analysis.

Donor cell preparation for transplantation

BM transplantation was performed to create chimeric mice with hematopoietic cells from VIP-KO donors or WT donors (control). Femora, tibia, and spleens were obtained from VIP-KO or WT mice. BM cells were harvested by flushing the specimens with sterile RPMI 1640 containing 1% heat-inactivated FCS. T cells were purified from splenocytes by negative selection using a mixture of biotinylated non-T cell Abs (anti-CD11b, B220, DX5, and Ter^{119}), streptavidin microbeads, and immunomagnetic separation (MACS; Miltenyi Biotec, Auburn, CA). The average purity of CD3$^+$ T cells was 95%. Lineage$^-$ (CD3, CD4, CD8, Gr-1, CD11b, I-A^b, DX5, B220, TER^{119}, and CD19) c-kit$^+$ sca-1$^+$ hematopoietic stem cells (HSC) and lineage$^-$ (CD3, DX5, IgM, TER^{119}, and CD19) CD11c$^+$ DC from donor BM were purified using a BD Biosciences FACS Aria cell sorter (36). Purity of FACS-purified HSC and DC averaged 93 and 97%, respectively.

Radiation chimeras and stem cell transplantation

On day −1, 8- to 10-wk-old male B6 CD45.1 congenic mice were irradiated with two fractions of 5.5 Gy for a total of 11 Gy (40). On day 0, irradiated mice received 5×10^6 T cell–depleted BM cells plus 3×10^5 MACS-purified splenic T cells via tail vein injection. Some experiments used an alternate approach, transplanting a combination of 5×10^3 HSC, 5×10^4 DC, plus 3×10^5 T cells. Mice were monitored for signs of severe infection, including fur texture, posture, activity, skin integrity, and weight loss. Each transplant group was followed for at least 100 d (41). Donor cell chimerism in peripheral blood was determined 2 mo after transplantation, and was typically ≥95%. Chimeric mice were then used in vaccination and mCMV infection studies.

Virus and immunization

The Smith strain of mCMV passaged in vivo in salivary glands and was frozen in aliquots in liquid nitrogen (37, 39). WT and VIP-KO mice, as well as chimeric mice with hematopoietic cells from WT and VIP-KO donors, were given either 5×10^4 (10% lethal dose; low-dose) or 1×10^5 (LD_{50}; high-dose) PFU mCMV by i.p. injection and then monitored for signs of illness, including hunched posture, decreased activity, and weight loss. Mice were vaccinated i.p. with 1×10^6 CFU Lm-mCMV, a *L. monocytogenes* that has been rendered nonpathogenic by knockout of bacterial genes associated with virulence (42) and engineered to express the mCMV H-2D^b restricted immunodominant peptide M45 aa 985–993 HGIRNASFI (43). The vaccine was prepared and supplied by Cerus (Concord, CA) (37, 38).

Analysis of peripheral blood and spleen samples

Blood and spleen samples were obtained on 3, 7, 10, 14, 17, and 21 d after vaccination or following mCMV infection. Leukocytes, RBCs, and platelets were counted using a Beckman Coulter automated counter. Blood and spleen samples were depleted of RBCs by ammonium chloride lysis and washed twice. NK, NK-T, and T cell subsets were enumerated using CD3 PE/PE-Cy7/FITC, CD4 PE-Alexa610/PE-Alexa700, CD8 PE-Cy7/PerCP, CD62L FITC/allophycocyanin, CD25 allophycocyanin-Cy7, CD44 PE-Cy5, CD69 PE-Cy7, programmed death-1 (PD-1) PE, and NK1.1 PE (BD Pharmingen, San Jose, CA). Cells were stained with mAbs specific for congenic markers CD45.2, CD45.1, CD90.1, and CD90.2 to determine donor chimerism. Allophycocyanin-labeled mCMV M45 aa 985–993 peptide-HGIRNASFI-H-2D^b tetramer was obtained from the Emory Tetramer Core Facility. All samples were analyzed on a FACS Canto (BD Biosciences, San Jose, CA), and list mode files were analyzed using FlowJo software (Tree Star 2007). Samples for flow cytometric analysis of mCMV-M45 epitope peptide–MHC-I tetramer$^+$ CD8$^+$ T cells (tetramer$^+$ CD8 T cells) were gated for lymphocytes in the area of forward and side light scatter, setting a gate for tetramer$^+$ T cells such that 0.01% of control (nonimmune) CD8$^+$ T cells were positive (37, 39). Flow cytometric analyses of the T regulatory-associated molecule PD-1 (44), the costimulatory molecule ICOS, the adhesion molecule CD62L (45), activation markers CD25 and CD69 (36, 46), intracellular cytokines (IFN-γ, TNF-α, IL-4, and IL-10), and DC markers (I-A^b, CD80, and programmed death ligand-1 [PD-L1]) were analyzed, as previously described (36).

In vivo killing assay

Naive splenocytes were harvested from CD45.1$^+$/CD45.2$^+$ heterozygous C57BL/6 mice and pulsed with 3 μM mCMV M45 aa 985–993 HGIRNASFI peptide in RPMI 1640 containing 3% FBS for 90 min at 37°C, and washed three times with ice-cold media. mCMV peptide-pulsed target splenocytes and nonpulsed splenocytes from CD45.1$^+$ B6 congenic mice were mixed together in equal parts, and 40×10^6 total target cells per mouse were injected i.v. into CD45.2$^+$ VIP-KO or WT C57BL/6 mice that had been infected 9 d earlier with low-dose (10% lethal dose) mCMV, or injected into noninfected WT control mice. Sixteen hours following injection of target cells, recipients were sacrificed, splenocytes harvested, and the numbers of mCMV peptide-pulsed CD45.1$^+$/CD45.2$^+$ and nonpulsed CD45.1$^+$ target cells were quantified by FACS analysis. Immune-mediated killing of mCMV peptide-pulsed targets was calculated by first dividing the percentage of peptide-pulsed or nonpulsed targets recovered

from the spleen of mCMV-immune mice with the mean percentage of the corresponding population of peptide-pulsed or nonpulsed targets from nonimmune mice (ratio of immune killing). The specific antiviral in vivo lytic activity for individual mice was calculated by the following formula: (1 − [ratio of immune killing mCMV peptide-pulsed target cells/ratio of immune killing nonpulsed target cells]) × 100.

In vitro measurements of immune responses to mCMV peptide

WT mice, VIP-KO mice, and mice engrafted with either WT or VIP-KO donor cells were infected with low-dose mCMV, and splenocytes were harvested 15 d later. Splenic DC and T cells were purified by FACS and MACS, respectively (36). DC were plated at 2×10^5 cells/ml in 12-well plates and centrifuged ($300 \times g$ for 30 min) with 3 μM mCMV peptide (37). After centrifugation, DC were washed three times with PBS, resuspended in complete medium, and incubated with 2×10^6 T cells at 37°C for 3 or 7 d (47). Cells were treated with Golgi Stop (BD Pharmingen) during the last 6 h of culture. Cells were then harvested from culture plates and stained with fluorescently labeled Abs against DC and T cell lineage markers (36), permeabilized, stained with Abs against IL-10 and IFN-γ, and analyzed by flow cytometry, as previously described, using isotype-matched control Abs to set the gates for distinguishing positive intracellular staining (36). Harvested culture media was stored at −20°C until use for cytokine analysis by ELISA (OptEIA ELISA sets for IL-10 and IFN-γ; BD Biosciences). ELISA plates were read using a SpectraMax 340PC spectrophotometer (Molecular Devices, Sunnyvale, CA) (36).

NK cell lytic activity

Lytic activity of NK cells was analyzed, as previously described (48). Briefly, YAC-1 cells, a sensitive target for NK cells, were labeled with 37 MBq $Na^{51}CrO_4$ at 37°C for 90 min and washed twice with warm RPMI 1640 medium. The labeled target cells (1×10^4) were cocultured with effector splenocytes (containing NK cells) at various ratios of effectors: targets (100:1, 50:1, and 25:1) in a final volume of 0.2 ml fresh medium in 96-well round-bottom microplates. The plates were incubated for 4 h at 37°C with 5% CO_2. The amount of ^{51}Cr released in 0.1 ml supernatant was measured by a well-type gamma counter (beta liquid scintillation counter; EG&G Wallac, PerkinElmer, Ontario, Canada). Specific cytotoxicity was calculated as follows: % ^{51}Cr release = 100 × (cpm experimental − cpm spontaneous release)/(cpm maximum release − cpm spontaneous release).

Determination of liver viral load

Viral load was analyzed, as previously described (39). Briefly, livers were collected from CMV-infected recipients, homogenized, and centrifuged. Serially diluted supernatants were added to 3T3 confluent monolayers in 24-well tissue culture plates and incubated for 90 min at 37°C and 5% CO_2, then overlayered with 1 ml 2.5% methylcellulose in DMEM, and returned to the incubator. After 4 d, the methylcellulose was removed and the 3T3 confluent monolayers were stained with methylene blue. mCMV plaques were directly counted under a light microscope (Nikon, Melville, NY). PFUs were calculated.

Statistical analyses

The data were analyzed using SPSS version 18 for MAC. In this study, each treatment group (or time point) had four to five mice, and every experiment was repeated at least twice. Data are presented as mean ± SD of all evaluable samples if not specified. Survival differences among groups were calculated with the Kaplan-Meier log-rank test in a pairwise fashion. Differences in tetramer response, cytokine levels, and T cell numbers were compared using a two-tailed Student *t* test. A *p* value <0.05 was considered significant.

Results

VIP-KO mice were resistant to mCMV infection

We first compared the hematological and immunological phenotypes of VIP-KO mice. We found no significant differences comparing blood from naive WT and VIP-KO mice in the numbers of total leukocytes, CD4, CD8, αβ TCR T cells, γδ T cells, B cells, myeloid leukocytes, and DCs in blood (Supplemental Fig. 1). VIP-KO and WT mice were infected with a nonlethal dose of mCMV (5×10^4 PFU) and sacrificed 3, 10, and 17 d later. VIP-KO mice had significantly less virus in their liver, a target for mCMV infection (37, 49), with more rapid clearance of virus than mCMV-infected WT mice ($p < 0.001$; Fig. 1). To test whether VIP-KO mice had better survival following mCMV infection, VIP-KO and WT mice were infected i.p. with either 1×10^5 PFU /mouse (high-dose) or 5×10^4 PFU/mouse (low-dose) mCMV. All WT mice given high-dose mCMV died by day 10 postinfection compared with 65% survival of the VIP-KO mice ($p < 0.001$; Fig. 2*A*). Following low-dose mCMV infection, both WT and VIP-KO mice had transient lethargy and weight loss, with recovery to baseline values by day 20 postinfection, with 100% of WT mice and 92% of VIP-KO mice surviving to day 100 postinfection (Fig. 2*A*, 2*B*). In a parallel experiment, serial measurements of CD4 and CD8 T cells following mCMV infection showed that VIP-KO mice had more $CD4^+$ and $CD8^+$ T cells in their blood and spleen compared with WT mice (Fig. 2*C–F*).

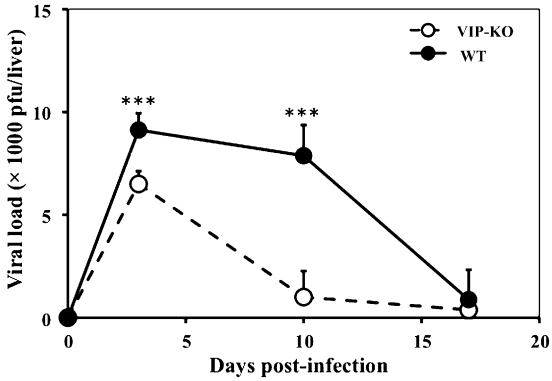

FIGURE 1. Mice lacking VIP had lower levels of virus in the liver following mCMV infection. VIP-KO (12–15 mice per time point, from 3 replicate experiments) and WT mice (12–15 mice per time point, from 3 replicate experiments) were infected (day 0) with low-dose 5×10^4 PFU mCMV. Livers were collected and weighed, and lysates were prepared at days 3, 7, 10, 14, and 17 d post-mCMV infection. Day 0 control livers were from uninfected mice ($n = 3$). Mean liver viral load was measured by plaque assay of a defined quantity of liver lysate on 3T3 cell monolayers, and the number of PFU/liver was calculated. ***$p < 0.001$, denoting a significant difference between VIP-KO and WT mice.

Innate and adaptive antiviral responses were enhanced in the absence of VIP

VIP-KO mice had significantly higher percentages (Fig. 3*A*) and absolute numbers of Ag-specific $tetramer^+$ CD8 T cells in the blood (Fig. 3*B*) and spleen (Fig. 3*C*) following low-dose mCMV infection than WT mice. The highest frequency of $tetramer^+$ CD8 T cells in the blood was seen on day +10 postinfection with 9.1 ± 0.8% of blood $CD8^+$ T cells in VIP-KO mice versus 4.8 ± 0.7% of blood $CD8^+$ T cells in WT mice ($p < 0.001$; Fig. 3*A*). Because lethality was 100% in WT mice receiving high-dose mCMV compared with 35% mortality among VIP-KO mice ($p < 0.001$), a longitudinal comparison of the numbers of Ag-specific T cells in WT versus VIP-KO mice could not be performed, but analysis at day 3 showed that VIP-KO mice had greater numbers of $tetramer^+$ CD8 T cells (295/ml ± 40/ml) compared with WT mice (124/ml ± 38/ml, $p < 0.001$). Enhanced innate antiviral immunity among VIP-KO mice was evidenced by higher levels of NK-mediated cytotoxicity against YAC1 targets in VIP-KO splenocytes harvested 3 d postinfection (Fig. 3*D*). Using mCMV peptide-pulsed and nonpulsed congenic splenocytes as targets in an in vivo cytotoxicity assay in immune mice (previously infected with low-dose mCMV), the specific lysis of mCMV peptide-pulsed targets was significantly enhanced in VIP-KO mice compared with WT mice (Fig. 4). Significantly, VIP-KO mice had similar baseline numbers, but more IFN-γ–expressing NK, NKT cells, and Th1/

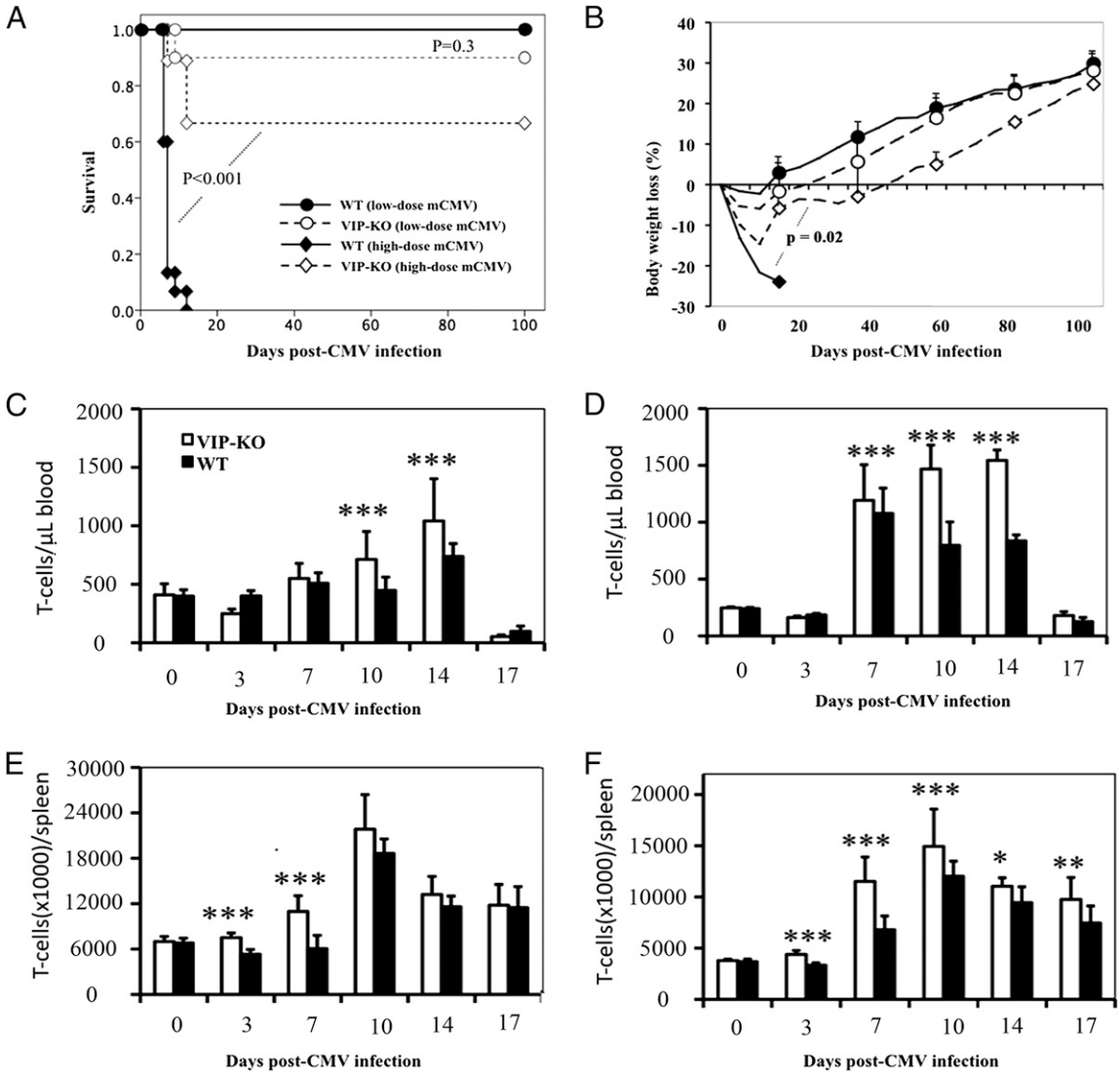

FIGURE 2. Mice lacking VIP had better survival and greater expansion of blood T cells following mCMV infection. VIP-KO and WT mice were infected (day 0) with low-dose 5×10^4 PFU or high-dose 1×10^5 PFU mCMV. Survival was recorded every day, and body weight was recorded twice weekly. Peripheral blood and spleen were collected baseline, prior to mCMV infection, and 3, 7, 10, 14, and 17 d postinfection. Blood cells and splenocytes were stained with fluorescently conjugated mAbs to CD45.2, CD3, CD4, and CD8, and analyzed by flow cytometry, and absolute numbers of cells/ml blood or per spleen were calculated. Data from 12–15 mice per group were pooled from 3 replicate experiments. *A* and *B*, Survival and body weight change of WT and VIP-KO mice that received graded doses of 5×10^4, or 1×10^5 PFU mCMV. *C* and *D*, Total numbers of $CD4^+$ and $CD8^+$ T cells in blood following low-dose mCMV infection. *E* and *F*, Total numbers of $CD4^+$ and $CD8^+$ T cells in the spleen following low-dose mCMV infection. $*p < 0.05$, $**p < 0.01$, $***p < 0.001$, denoting a significant difference between VIP-KO and WT mice.

Tc1-polarized (IFN-γ^+ and TNF-α^+) T cells on days 3–17 post-infection compared with WT mice (Supplemental Fig. 2*A–H*).

The absence of VIP expression in donor hematopoietic cells enhanced antiviral immunity in radiation hematopoietic chimeras

Because VIP is expressed in multiple cell lineages (2–6), we tested whether mice lacking VIP expression only in their hematopoietic cells had the same level of enhanced antiviral immunity as we observed in VIP-KO mice. We used VIP-KO mice as donors of hematopoietic cells and created radiation chimeras with syngenic BM transplantation in which recipients had >95% donor cell engraftment (36). The day 59 survival of mice transplanted with VIP-KO 3×10^3 FACS-purified HSC, 5×10^4 FACS-purified DC, and 3×10^5 MACS-purified T cells (75 ± 10%) was similar to the survival seen among mice transplanted with WT HSC, DC, and T cells (80 ± 9%). To explore the effect of VIP expression in hematopoietic cells on primary and secondary immune responses, VIP-KO→WT and WT→WT syngeneic transplant recipients were primed with PBS or the Lm-mCMV vaccine (containing mCMV immunodominant M45 epitope peptide aa 985–993), followed by infection 21 d later with low-dose mCMV (Fig. 5). Peripheral blood samples obtained prior to Lm-mCMV vaccination (day 59 posttransplant), after vaccination, and following mCMV infection (day 80 posttransplant) were analyzed for the numbers of tetramer$^+$ CD8 T cells. Nonimmunized WT and VIP-KO chimeric mice had minimal numbers of mCMV-peptide tetramer$^+$ CD8 T cells in their blood at baseline (Fig. 5*A*). Following primary mCMV infection, recipients engrafted with VIP-KO hematopoietic cells had significantly more mCMV peptide tetramer$^+$ CD8 T cells in their blood compared with WT mice (Fig. 5*A*). Vaccination with Lm-mCMV led to a larger increase in blood mCMV tetramer$^+$ T cells in the VIP-KO→WT chimeras compared with WT→WT chimeras (Fig. 5*B*), indicating that mCMV peptide pre-

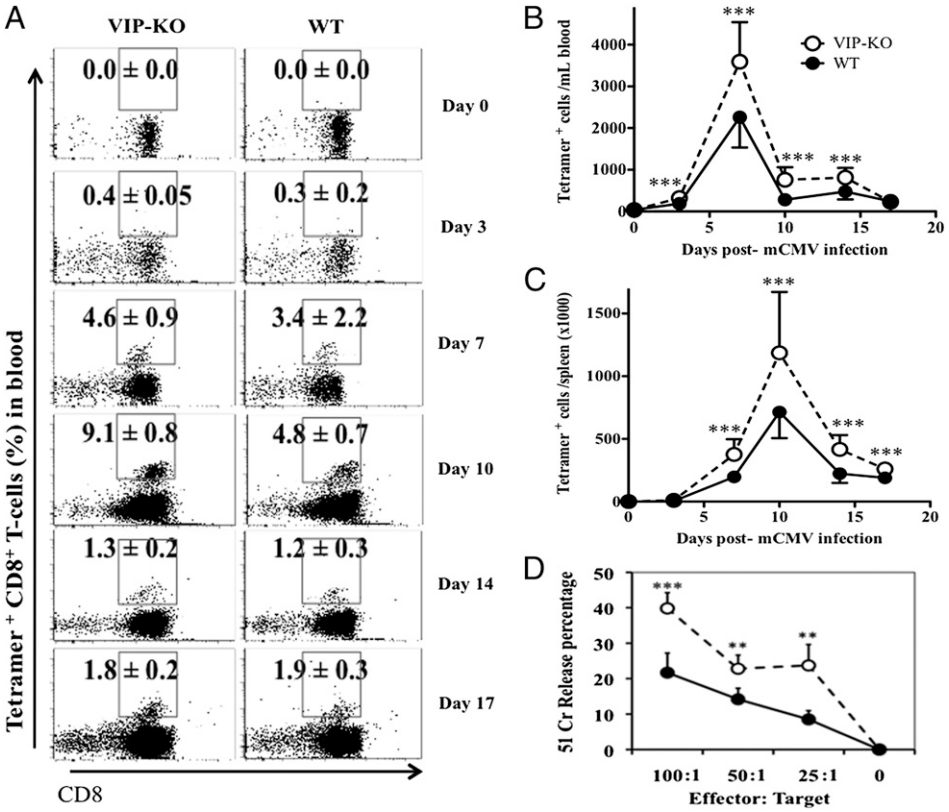

FIGURE 3. Mice lacking VIP had larger increases of Ag-specific T cells following mCMV infection. VIP-KO and WT mice were infected (day 0) with low-dose 5×10^4 PFU or high-dose 1×10^5 PFU mCMV. Peripheral blood and spleen were collected at baseline, prior to infection and 3, 7, 10, 14, and 17 d post-mCMV infection. Blood cells and splenocytes were stained with fluorescently conjugated mAbs to CD45.2, CD3, CD4, CD8, and mCMV M45-epitope peptide-specific MHC-I tetramer reagents and analyzed by flow cytometry, and absolute numbers of cells/ml blood and per spleen were calculated. NK cell-killing activity was measured by ^{51}Cr releasing assay using YAC-1–pulsed ^{51}Cr. *A*, Percentages of tetramer$^+$ CD8 T cells in blood following low-dose mCMV infection. Dot graphs showed concatenated list mode files from analysis of four mice per group 10 d following mCMV infection (mean ± SD), and are representative of five replicate experiments. *B*, Absolute numbers of tetramer$^+$ CD8 T cells/ml in blood following low-dose mCMV infection (data are from 5 replicate experiments involving a total of 12–20 mice per time point). *C*, Absolute numbers of tetramer$^+$ CD8 T cells in the spleen following low-dose mCMV infection (data are from 5 replicate experiments involving a total of 12–20 mice per time point). *D*, NK cells mediated cytolytic activity (data are from 3 replicate experiments with 12 mice per time point). $^{**}p < 0.01$, $^{***}p < 0.001$, denoting a significant difference between VIP-KO and WT mice.

sentation alone in VIP-KO mice (in the absence of viral infection) was sufficient to result in enhanced expansion of Ag-specific T cells. Subsequent infection of the Lm-mCMV–vaccinated mice with low-dose mCMV led to an accelerated anamnestic response in VIP-KO→WT chimeras compared with mice engrafted with WT BM (Fig. 5*B*). Because both T cells and accessory cells can secrete VIP (4–6), we further explored the role of VIP synthesis by different immune cell subsets by creating radiation chimeras engrafted with the combination of donor DC and HSC from VIP-KO mice and donor T cells from WT mice. Mice transplanted with the heterogeneous combination of VIP-KO HSC and DC and WT T cells did not show the enhanced immune responses seen in mice engrafted with the homogeneous combination of VIP-KO HSC, DC, and T cells (Fig. 5*B*), indicating that VIP production by donor T cells was sufficient to attenuate antiviral cellular immunity.

Absence of VIP augmented antiviral CD8$^+$ T cell proliferation and Th1/Tc1 polarization in vitro

To study the effect of VIP on antiviral immunity in vitro, we analyzed cultures of T cells and mCMV peptide-pulsed DC for tetramer$^+$ CD8 T cells and for Th1 and Th2 cytokines. DC and T cells were purified from WT or VIP-KO mice (36), and the DC were pulsed with mCMV peptide, and then mixed with T cells. The numbers of tetramer$^+$ CD8 T cells generated over 10 d of culture were measured by flow cytometry. Significantly greater numbers of Ag-specific tetramer$^+$ CD8 T cells were detected after 3 d in cultures of T cells with DC that had been isolated from mCMV-immune VIP-KO mice compared with similar cells isolated from mCMV-immune WT mice (Fig. 6*A*). To rule out an effect of VIP synthesized by nonhematopoietic cells on in vitro immune responses to mCMV peptides, donor-derived T cells and DC were recovered from syngeneic transplant recipients of VIP-KO→WT or WT→WT radiation chimeras. Homogeneous cultures of DC and T cells recovered from VIP-KO→WT radiation chimera generated more tetramer$^+$ CD8 T cells than cultures of DC and T cells from WT→WT radiation chimeras (Fig. 6*B*), indicating the absence of VIP synthesis by hematopoietic cells in radiation chimeras programmed T cells and DC toward enhanced cellular immune responses. Supernatants from cultures of T cells and mCMV peptide-pulsed DC from WT mice had higher levels of IL-10, and lower levels of IFN-γ compared with supernatants from cultures of T cells and mCMV peptide-pulsed DC from VIP-KO mice (Fig. 6*C*, 6*D*). To determine whether synthesis of VIP by T cells was sufficient to downregulate immune responses to mCMV, we cultured WT T cells and VIP-KO DC isolated from radiation chimeras originally transplanted with the heterogeneous combination of WT T cells plus VIP-KO DC and VIP-KO HSC. In contrast to the larger numbers of tetramer$^+$ CD8 T cells seen in homogeneous cultures of T cells and DC from VIP-KO mice, heterogeneous cultures of WT

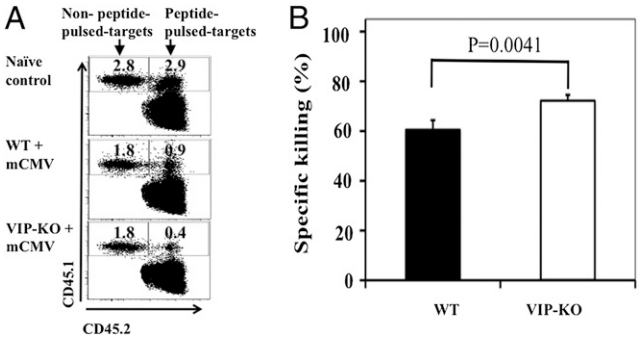

FIGURE 4. VIP-KO mice had increased cytolytic activity against M45 peptide-pulsed targets following mCMV infection. A mixture of peptide-pulsed targets ($CD45.1^+$ $CD45.2^+$) and nonpulsed targets ($CD45.2^-$ $CD45.1^+$) was adoptively transferred to VIP-KO and WT mice 9 d post-infection with low-dose mCMV. Target cells were harvested from the recipient spleens 16 h after i.v. injection, and peptide-pulsed targets and nonpulsed targets were differentiated by flow cytometry following staining for CD45 congenic markers. *A*, A representative flow cytometry analysis plot of splenocytes from recipient mice showing mean percentages of peptide-pulsed target cells and nonpulsed target cells. Dot graphs showed concatenated list mode files from analysis of five mice per group. *B*, Calculated mean specific cytolytic activity, $n = 5$, representative of two replicate experiments.

T cells plus VIP-KO DC generated fewer $tetramer^+$ CD8 T cells, similar to cultures of WT T cells and WT DC, indicating that VIP synthesis by T cells acts as a dominant-negative regulatory mechanism in antiviral cellular immunity in vitro (Fig. 6*B*).

VIP-KO mice had higher levels of costimulatory molecule and MHC-II expression on DC and less PD-1/PD-L1 expression compared with WT mice following mCMV infection

To explore the mechanism by which the absence of VIP enhanced antiviral immunity, we studied the expression of costimulatory molecules and PD-1/PD-L1 expression in WT and VIP-KO mice following mCMV infection. Prior to mCMV infection, baseline levels of MHC-II, CD80, and PD-L1 expression on DCs, and PD-1 expression on CD4 and CD8 T cells were similar comparing WT with VIP-KO mice (Fig. 7). VIP-KO mice had a marked upregulation of CD80 and MHC-II expression on cDC and pDC 3 d after mCMV infection compared with the corresponding DC subsets from mCMV-infected WT mice. Of note, the absence of VIP expression had a significant impact on the upregulation of coinhibitory molecules and ligands that normally follows mCMV infection: PD-L1 expression was upregulated 3 d after mCMV infection in DC from WT, but not VIP-KO mice, whereas WT $CD8^+$ T cells showed a striking upregulation of PD-1 expression on day 10 after mCMV infection that was not seen in $CD8^+$ T cells from VIP-KO mice (Fig. 7).

Discussion

In this study, we explored the immunoregulatory effect of VIP in immune responses to mCMV infection, hypothesizing that the absence of VIP would increase innate and adaptive immune responses to viral infection. Our data using VIP-KO mice demonstrate that the absence of physiological levels of VIP in hematopoietic cells led to striking enhancement of innate and adaptive antiviral cellular immune responses. VIP-KO mice had less mortality and faster viral clearance compared with WT mice. The increased expansion of $tetramer^+$ CD8 T cells and increased cytolytic activity of NK cells seen in VIP-KO mice are most likely responsible for their greater resistance to mCMV infection (50). Whereas we used the M45 epitope peptide to measure mCMV-specific T cells, and T cells recognizing this epitope have been shown to be relatively ineffective in clearing virus-infected cells due to m152/gp40–mediated immune interference (51), the enhanced killing of M45 epitope-containing peptide-pulsed target cells supports the contribution of M45-reactive T cells to functional antiviral cytotoxic activity in vivo.

To clarify the effect of various physiological sources of VIP (hematopoietic versus neuronal), we used C57BL/6 radiation chimeras engrafted with syngeneic VIP-KO or WT hematopoietic cells following myeloablative radiation. Recipients of VIP-KO hematopoietic grafts showed accelerated kinetics of cellular immune responses to primary mCMV infection and Lm-mCMV vaccination, as well as greater amnestic responses following Lm-mCMV vaccination and mCMV infection compared with recipients of WT grafts. These data indicate that VIP produced by hematopoietic cells has a dominant-negative effect on antiviral cellular immune responses, and that VIP synthesis by non-hematopoietic neuronal cells does not significantly affect antiviral immune responses in this system.

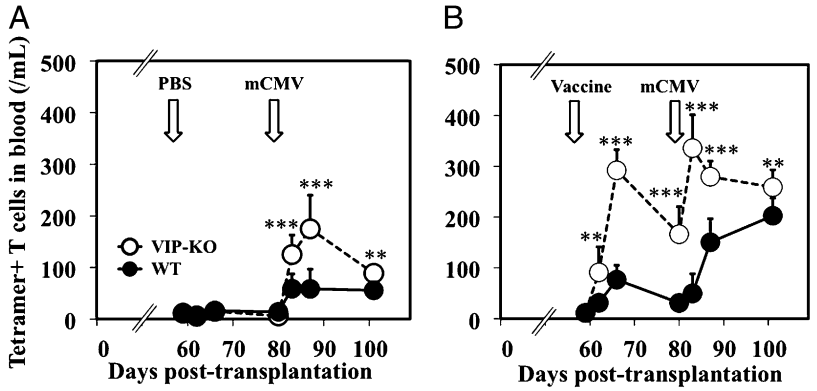

FIGURE 5. Radiation chimeras engrafted with hematopoietic cells from VIP-KO donors had enhanced primary and secondary Ag-specific cellular immune responses following Lm-mCMV vaccination and mCMV infection. Syngeneic BM chimeric mice were generated by transplanting lethally irradiated $H\text{-}2K^b$ recipients with 3×10^3 HSC, 5×10^4 DC, and 3×10^5 T cells from either VIP-KO or WT $H\text{-}2K^b$ donor mice. Fifty-nine days posttransplant, mice were vaccinated with 1×10^6 CFU Lm-mCMV or PBS, and then 80 d posttransplant, mice were infected with low-dose 5×10^4 PFU mCMV. Blood samples were collected at days 59, 62, 66, 80, 83, 87, and 101 posttransplantation and analyzed by flow cytometry for $tetramer^+$ CD8 T cells. Data represent mean values of 12–16, per time point, pooled from three replicate experiments. *A*, Mice were treated first with PBS, and then infected with mCMV. *B*, Primary and secondary immune responses in mice following vaccination with Lm-mCMV and then infection with low-dose mCMV. $^{**}p < 0.01$, $^{***}p < 0.001$ comparing $tetramer^+$ T cell levels between mice transplanted with VIP-KO hematopoietic cells and WT hematopoietic cells.

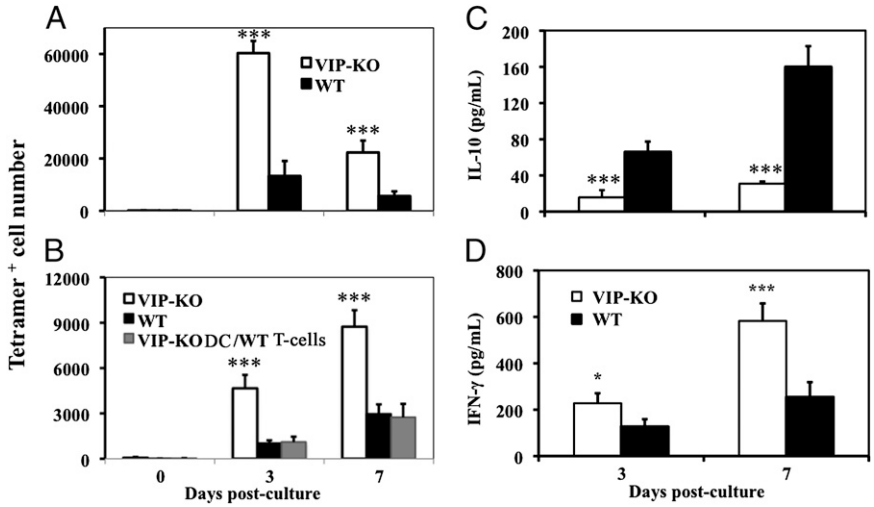

FIGURE 6. The generation of Ag-specific antiviral T cells and Th1 polarization was increased in cultures of DC and T cells from VIP-KO mice compared with cells from WT mice. DC and T cells were isolated from spleens of VIP-KO and WT mice, and from radiation chimeric mice that received homogeneous grafts from VIP-KO or WT (3×10^3) HSC, (5×10^4) DC and (1×10^6) T cells, and heterogeneous grafts from the combination of VIP-KO HSC and DC and WT T cells 15 d following infection with 5×10^4 PFU (low-dose) mCMV (15–18 per group were studied). FACS-purified DC from these mice were incubated with 3 μM mCMV peptide for 30 min, washed, and then triple-well cocultured with T cells from the same groups. On days 3 and 7 of culture, Ag-specific T cells were measured by FACS using mCMV-M45 epitope peptide–MHC-I tetramer reagent. *A* and *B*, The absolute numbers of tetramer$^+$ CD8 T cells/ml in cultures of cells from nontransplanted (*A*) and radiation chimeric mice (*B*). Day 0 data were obtained using cells from noninfected mice. Culture media from day 3 cultures of cells from radiation chimeric mice were assayed for IL-10 (*C*) and IFN-γ (*D*) by ELISA. $*p < 0.05$, $***p < 0.001$, comparing VIP-KO mice and WT groups. Means ± SE from pooled results of three repeat experiments. The experiment was repeated three times.

Immune cells in VIP-KO mice had more Th1 polarization (52, 53), less Th2 polarization, and higher MHC-II expression (47) than those of WT mice following mCMV infection, consistent with the reports that VIP is a negative regulator of Th1 immune responses (3, 54). A simple in vitro model of T cells cocultured with mCMV peptide-pulsed DC recapitulated the in vivo immunology of VIP-KO mice. Cocultures of DC and T cells from VIP-KO mice had higher levels of IFN-γ^+ CD4$^+$ and CD8$^+$ T cells and more Ag-specific antiviral CD8$^+$ T cells compared with cultures of WT DC and WT T cells. Conditioned media from cultures of WT

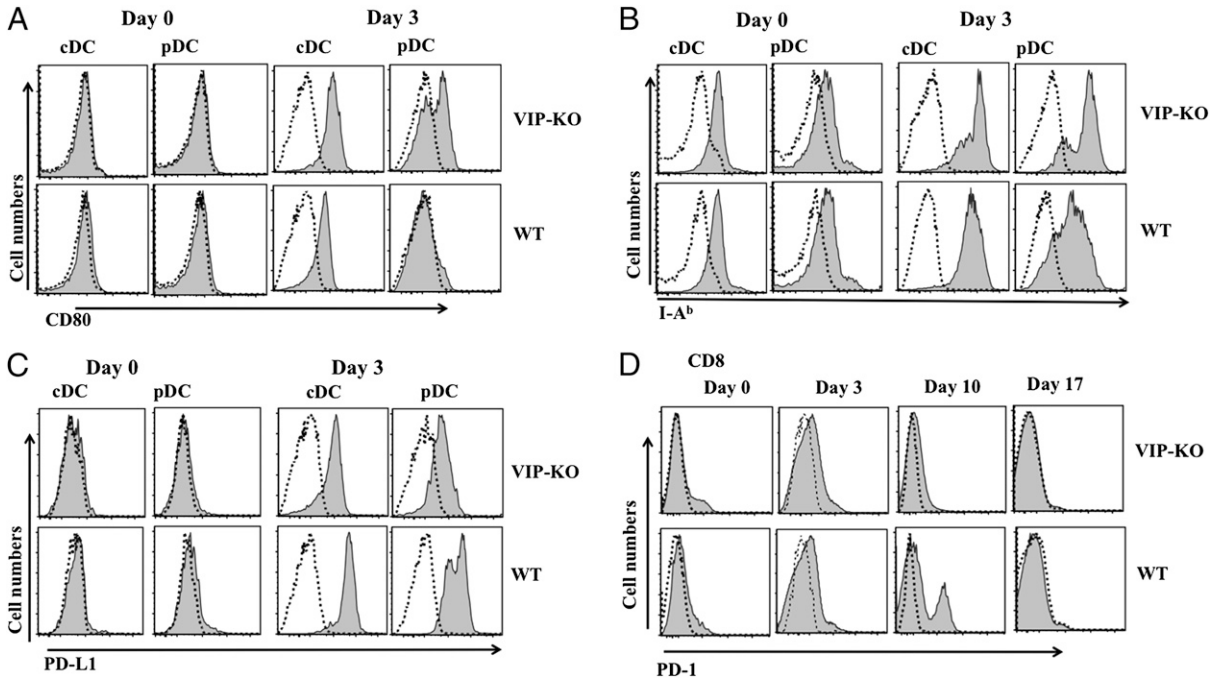

FIGURE 7. Higher levels of CD80 and MHC-II expression on DC and lower levels of PD-1 and PD-L1 expression on CD8$^+$ T cells and DC, respectively, from VIP-KO mice following mCMV infection. Splenocytes were isolated from VIP-KO and WT mice at baseline and 3, 10, and 17 d postinfection with 5×10^4 PFU mCMV. Expression patterns of CD80 (*A*), MHC-II (*B*), and PD-L1 (*C*) on conventional DC (cDC, lineage$^-$, CD11c^{high}, B220$^-$) and plasmacytoid DC (pDC, lineage$^-$, CD11c^{low}, B220$^+$) and the percentages of CD8$^+$ T cells expressing PD-1 (*D*) were analyzed by flow cytometry. Histograms depict analysis of concatenated list mode files from four mice per group at each time point, and are representative of three replicate experiments. Dashed lines represent the staining profile using an isotype-matched control Ab; filled lines represent specific staining.

T cells and WT DC had higher levels of IL-10, and lower levels of IFN-γ, compared with culture media from VIP-KO T cells and VIP-KO DC, consistent with other reports (55). Heterogeneous cocultures of VIP-KO DC and WT T cells had the same (lower) numbers of Ag-specific antiviral $CD8^+$ T cells as cultures of WT DC and WT T cells, confirming that T cells making VIP are sufficient to polarize Th2 immunity and suppress Th1 immunity, and that VIP made by T cells is a dominant-negative regulator of antiviral immune responses (56, 57).

The mechanisms for the enhanced antiviral cellular immunity and greater Th1/Tc1 immune polarization seen in VIP-KO mice following mCMV infection appear to be due to a profound shift in the pattern of costimulatory and coinhibitory molecule expression on DC and $CD8^+$ T cells. The higher levels of MHC-II and CD80 on cultured VIP-KO DC compared with WT DC are consistent with previous reports that mature DC activate Th1 immune responses (36, 58) and that supraphysiological levels of VIP induce tolerogenic DC that express lower levels of costimulatory molecules (12). Another possible mechanism is that VIP signaling interferes with the ability of the mCMV protein m138 to target CD80 expression on DC (59). An important new finding in this study is that VIP modulates the expression of the PD-1 and PD-L1 coinhibitory molecules that regulate immune polarization and survival of T cells. PD-L1–PD-1 interactions are known to regulate the initial priming of naive T cells by mCMV-infected APC, and are distinct from the role that PD-1 signaling plays in T cell "exhaustion" described for several persistent/chronic viral infections in humans and mice (60), including hCMV (61). Following viral infection, upregulation of the PD-L1/L2–PD-1 pathway has been associated with immunosuppression (62) due to cell cycle arrest and death of T cells, either through the direct engagement of a death pathway or indirectly by downregulating survival signals and growth factors (61). PD-L1/L2 expression on DC is associated with reduced expression of CD40, CD80, and CD86 and increased IL-10 production (63). We found that DC from mice transplanted with VIP-KO cells had dramatically reduced PD-L1 expression on DC and PD-1 expression on activated memory $CD8^+$ T cells that were associated with increased quantitative and qualitative antiviral T cell responses following mCMV infection. Our studies indicate that physiological levels of VIP contribute to the upregulation of PD-L1/PD-1 expression seen in WT mice following mCMV infection. This work further suggests that induction of VIP may be part of the active suppression of adaptive immune responses that occurs following mCMV infection.

In summary, these data indicate that VIP synthesis by hematopoietic cells is a key factor in regulating the development of protective Th1 immune responses following vaccination or infection with mCMV. The absence of VIP synthesis by hematopoietic cells leads to lower levels of counter-regulatory coinhibitory molecules and changes in serum cytokines consistent with global Th1 immune polarization. The increased antiviral immunity seen in the absence of VIP suggests that VIP antagonists may be of clinical benefit for patients with viral infection.

Disclosures

The authors have no financial conflicts of interest.

References

1. Varela, N., A. Chorny, E. Gonzalez-Rey, and M. Delgado. 2007. Tuning inflammation with anti-inflammatory neuropeptides. *Expert Opin. Biol. Ther.* 7: 461–478.
2. Fahrenkrug, J. 1979. Vasoactive intestinal polypeptide: measurement, distribution and putative neurotransmitter function. *Digestion* 19: 149–169.
3. Delgado, M., D. Pozo, and D. Ganea. 2004. The significance of vasoactive intestinal peptide in immunomodulation. *Pharmacol. Rev.* 56: 249–290.
4. Gomariz, R. P., M. Delgado, J. R. Naranjo, B. Mellström, A. Tormo, F. Mata, and J. Leceta. 1993. VIP gene expression in rat thymus and spleen. *Brain Behav. Immun.* 7: 271–278.
5. Lygren, I., A. Revhaug, P. G. Burhol, K. E. Giercksky, and T. G. Jenssen. 1984. Vasoactive intestinal polypeptide and somatostatin in leucocytes. *Scand. J. Clin. Lab. Invest.* 44: 347–351.
6. Leceta, J., M. C. Martinez, M. Delgado, E. Garrido, and R. P. Gomariz. 1994. Lymphoid cell subpopulations containing vasoactive intestinal peptide in the rat. *Peptides* 15: 791–797.
7. Abad, C., P. Niewiadomski, D. Loh, and J. A. Waschek. 2006. Neurotransmitter and immunomodulatory actions of VIP and PACAP: lessons from knockout mice. *Int. J. Pept. Res. Ther.* 12: 297–310.
8. Girard, B. A., V. Lelievre, K. M. Braas, T. Razinia, M. A. Vizzard, Y. Ioffe, R. El Meskini, G. V. Ronnett, J. A. Waschek, and V. May. 2006. Noncompensation in peptide/receptor gene expression and distinct behavioral phenotypes in VIP- and PACAP-deficient mice. *J. Neurochem.* 99: 499–513.
9. Chorny, A., E. Gonzalez-Rey, A. Fernandez-Martin, D. Ganea, and M. Delgado. 2006. Vasoactive intestinal peptide induces regulatory dendritic cells that prevent acute graft-versus-host disease while maintaining the graft-versus-tumor response. *Blood* 107: 3787–3794.
10. Lara-Marquez, M., M. O'Dorisio, T. O'Dorisio, M. Shah, and B. Karacay. 2001. Selective gene expression and activation-dependent regulation of vasoactive intestinal peptide receptor type 1 and type 2 in human T cells. *J. Immunol.* 166: 2522–2530.
11. Delgado, M., E. Gonzalez-Rey, and D. Ganea. 2005. The neuropeptide vasoactive intestinal peptide generates tolerogenic dendritic cells. *J. Immunol.* 175: 7311–7324.
12. Delgado, M. 2009. Generating tolerogenic dendritic cells with neuropeptides. *Hum. Immunol.* 70: 300–307.
13. Delgado, M., R. P. Gomariz, C. Martinez, C. Abad, and J. Leceta. 2000. Anti-inflammatory properties of the type 1 and type 2 vasoactive intestinal peptide receptors: role in lethal endotoxic shock. *Eur. J. Immunol.* 30: 3236–3246.
14. Gomariz, R. P., A. Arranz, Y. Juarranz, I. Gutierrez-Cañas, M. Garcia-Gomez, J. Leceta, and C. Martínez. 2007. Regulation of TLR expression, a new perspective for the role of VIP in immunity. *Peptides* 28: 1825–1832.
15. Arranz, A., Y. Juarranz, J. Leceta, R. P. Gomariz, and C. Martínez. 2008. VIP balances innate and adaptive immune responses induced by specific stimulation of TLR2 and TLR4. *Peptides* 29: 948–956.
16. Lee, H., K. Park, J. S. Kim, and S. J. Lee. 2009. Vasoactive intestinal peptide inhibits Toll-like receptor 3-induced nitric oxide production in Schwann cells and subsequent sensory neuronal cell death in vitro. *J. Neurosci. Res.* 87: 171–178.
17. Herrera, J. L., E. Gonzalez-Rey, R. Fernandez-Montesinos, F. J. Quintana, R. Najmanovich, and D. Pozo. 2009. Toll-like receptor stimulation differentially regulates vasoactive intestinal peptide type 2 receptor in macrophages. *J. Cell. Mol. Med.* 13: 3209–3217.
18. Hudson, J. B. 1979. The murine cytomegalovirus as a model for the study of viral pathogenesis and persistent infections. *Arch. Virol.* 62: 1–29.
19. Jordan, M. C., and J. L. Takagi. 1983. Virulence characteristics of murine cytomegalovirus in cell and organ cultures. *Infect. Immun.* 41: 841–843.
20. Tortorella, D., B. E. Gewurz, M. H. Furman, D. J. Schust, and H. L. Ploegh. 2000. Viral subversion of the immune system. *Annu. Rev. Immunol.* 18: 861–926.
21. Rawlinson, W. D., H. E. Farrell, and B. G. Barrell. 1996. Analysis of the complete DNA sequence of murine cytomegalovirus. *J. Virol.* 70: 8833–8849.
22. Chee, M. S., A. T. Bankier, S. Beck, R. Bohni, C. M. Brown, R. Cerny, T. Horsnell, C. A. Hutchison, III, T. Kouzarides, J. A. Martignetti, et al. 1990. Analysis of the protein-coding content of the sequence of human cytomegalovirus strain AD169. *Curr. Top. Microbiol. Immunol.* 154: 125–169.
23. Reddehase, M. J. 2002. Antigens and immunoevasins: opponents in cytomegalovirus immune surveillance. *Nat. Rev. Immunol.* 2: 831–844.
24. Lyons, P. A., P. B. Dallas, C. Carrello, G. R. Shellam, and A. A. Scalzo. 1994. Mapping and transcriptional analysis of the murine cytomegalovirus homologue of the human cytomegalovirus UL103 open reading frame. *Virology* 204: 835–839.
25. Loh, L. C., W. J. Britt, C. Raggo, and S. Laferté. 1994. Sequence analysis and expression of the murine cytomegalovirus phosphoprotein pp50, a homolog of the human cytomegalovirus UL44 gene product. *Virology* 200: 413–427.
26. Li, W., K. Eidman, R. C. Gehrz, and B. Kari. 1995. Identification and molecular characterization of the murine cytomegalovirus homolog of the human cytomegalovirus UL100 gene. *Virus Res.* 36: 163–175.
27. Heise, M. T., and H. W. Virgin IV. 1995. The T-cell-independent role of gamma interferon and tumor necrosis factor alpha in macrophage activation during murine cytomegalovirus and herpes simplex virus infections. *J. Virol.* 69: 904–909.
28. Orange, J. S., B. Wang, C. Terhorst, and C. A. Biron. 1995. Requirement for natural killer cell-produced interferon gamma in defense against murine cytomegalovirus infection and enhancement of this defense pathway by interleukin 12 administration. *J. Exp. Med.* 182: 1045–1056.
29. Quinnan, G. V., J. E. Manischewitz, and F. A. Ennis. 1978. Cytotoxic T lymphocyte response to murine cytomegalovirus infection. *Nature* 273: 541–543.
30. Selgrade, M. K., Y. S. Huang, J. A. Graham, C. H. Huang, and P. C. Hu. 1983. Humoral antibody response to individual viral proteins after murine cytomegalovirus infection. *J. Immunol.* 131: 3032–3035.
31. Stoddart, C. A., R. D. Cardin, J. M. Boname, W. C. Manning, G. B. Abenes, and E. S. Mocarski. 1994. Peripheral blood mononuclear phagocytes mediate dissemination of murine cytomegalovirus. *J. Virol.* 68: 6243–6253.

32. Andrews, D. M., C. E. Andoniou, F. Granucci, P. Ricciardi-Castagnoli, and M. A. Degli-Esposti. 2001. Infection of dendritic cells by murine cytomegalovirus induces functional paralysis. *Nat. Immunol.* 2: 1077–1084.
33. Farrell, H. E., H. Vally, D. M. Lynch, P. Fleming, G. R. Shellam, A. A. Scalzo, and N. J. Davis-Poynter. 1997. Inhibition of natural killer cells by a cytomegalovirus MHC class I homologue in vivo. *Nature* 386: 510–514.
34. Farrell, H. E., M. A. Degli-Esposti, and N. J. Davis-Poynter. 1999. Cytomegalovirus evasion of natural killer cell responses. *Immunol. Rev.* 168: 187–197.
35. Colwell, C. S., S. Michel, J. Itri, W. Rodriguez, J. Tam, V. Lelievre, Z. Hu, X. Liu, and J. A. Waschek. 2003. Disrupted circadian rhythms in VIP- and PHI-deficient mice. *Am. J. Physiol. Regul. Integr. Comp. Physiol.* 285: R939–R949.
36. Li, J. M., L. T. Southerland, Y. Lu, K. A. Darlak, C. R. Giver, D. W. McMillin, W. A. Harris, D. L. Jaye, and E. K. Waller. 2009. Activation, immune polarization, and graft-versus-leukemia activity of donor T cells are regulated by specific subsets of donor bone marrow antigen-presenting cells in allogeneic hemopoietic stem cell transplantation. *J. Immunol.* 183: 7799–7809.
37. Hossain, M. S., J. D. Roback, F. Wang, and E. K. Waller. 2008. Host and donor immune responses contribute to antiviral effects of amotosalen-treated donor lymphocytes following early posttransplant cytomegalovirus infection. *J. Immunol.* 180: 6892–6902.
38. Hossain, M. S., J. D. Roback, B. P. Pollack, D. L. Jaye, A. Langston, and E. K. Waller. 2007. Chronic GvHD decreases antiviral immune responses in allogeneic BMT. *Blood* 109: 4548–4556.
39. Hossain, M. S., J. D. Roback, B. P. Pollack, D. L. Jaye, A. Langston, and E. K. Waller. 2007. Chronic GvHD decreases anti-viral immune responses in allogeneic BMT. *Blood* 109: 4548–4556.
40. Waller, E. K., A. M. Ship, S. Mittelstaedt, T. W. Murray, R. Carter, I. Kakhniashvili, S. Lonial, J. T. Holden, and M. W. Boyer. 1999. Irradiated donor leukocytes promote engraftment of allogeneic bone marrow in major histocompatibility complex mismatched recipients without causing graft-versus-host disease. *Blood* 94: 3222–3233.
41. Cooke, K. R., L. Kobzik, T. R. Martin, J. Brewer, J. Delmonte, Jr., J. M. Crawford, and J. L. Ferrara. 1996. An experimental model of idiopathic pneumonia syndrome after bone marrow transplantation. I. The roles of minor H antigens and endotoxin. *Blood* 88: 3230–3239.
42. Brockstedt, D. G., M. A. Giedlin, M. L. Leong, K. S. Bahjat, Y. Gao, W. Luckett, W. Liu, D. N. Cook, D. A. Portnoy, and T. W. Dubensky Jr. 2004. *Listeria*-based cancer vaccines that segregate immunogenicity from toxicity. *Proc. Natl. Acad. Sci. USA* 101: 13832–13837.
43. Gold, M. C., M. W. Munks, M. Wagner, U. H. Koszinowski, A. B. Hill, and S. P. Fling. 2002. The murine cytomegalovirus immunomodulatory gene m152 prevents recognition of infected cells by M45-specific CTL but does not alter the immunodominance of the M45-specific CD8 T cell response in vivo. *J. Immunol.* 169: 359–365.
44. Vignali, D. A., L. W. Collison, and C. J. Workman. 2008. How regulatory T cells work. *Nat. Rev. Immunol.* 8: 523–532.
45. Li, J. M., and E. K. Waller. 2004. Donor antigen-presenting cells regulate T-cell expansion and antitumor activity after allogeneic bone marrow transplantation. *Biol. Blood Marrow Transplant.* 10: 540–551.
46. Ziegler, S. F., F. Ramsdell, and M. R. Alderson. 1994. The activation antigen CD69. *Stem Cells* 12: 456–465.
47. Mathys, S., T. Schroeder, J. Ellwart, U. H. Koszinowski, M. Messerle, and U. Just. 2003. Dendritic cells under influence of mouse cytomegalovirus have a physiologic dual role: to initiate and to restrict T cell activation. *J. Infect. Dis.* 187: 988–999.
48. Salem, M. L., and M. S. Hossain. 2000. In vivo acute depletion of CD8(+) T cells before murine cytomegalovirus infection upregulated innate antiviral activity of natural killer cells. *Int. J. Immunopharmacol.* 22: 707–718.
49. Ebihara, K., and Y. Minamishima. 1984. Protective effect of biological response modifiers on murine cytomegalovirus infection. *J. Virol.* 51: 117–122.
50. Li, J. M., C. R. Giver, Y. Lu, M. S. Hossain, M. Akhtari, and E. K. Waller. 2009. Separating graft-versus-leukemia from graft-versus-host disease in allogeneic hematopoietic stem cell transplantation. *Immunotherapy* 1: 599–621.
51. Holtappels, R., J. Podlech, M. F. Pahl-Seibert, M. Jülch, D. Thomas, C. O. Simon, M. Wagner, and M. J. Reddehase. 2004. Cytomegalovirus misleads its host by priming of CD8 T cells specific for an epitope not presented in infected tissues. *J. Exp. Med.* 199: 131–136.
52. Gottfried-Blackmore, A., U. W. Kaunzner, J. Idoyaga, J. C. Felger, B. S. McEwen, and K. Bulloch. 2009. Acute in vivo exposure to interferon-gamma enables resident brain dendritic cells to become effective antigen presenting cells. *Proc. Natl. Acad. Sci. USA* 106: 20918–20923.
53. Steimle, V., C. A. Siegrist, A. Mottet, B. Lisowska-Grospierre, and B. Mach. 1994. Regulation of MHC class II expression by interferon-gamma mediated by the transactivator gene CIITA. *Science* 265: 106–109.
54. Gutiérrez-Cañas, I., Y. Juarranz, B. Santiago, C. Martínez, R. P. Gomariz, J. L. Pablos, and J. Leceta. 2008. Immunoregulatory properties of vasoactive intestinal peptide in human T cell subsets: implications for rheumatoid arthritis. *Brain Behav. Immun.* 22: 312–317.
55. Popkin, D. L., M. A. Watson, E. Karaskov, G. P. Dunn, R. Bremner, and H. W. Virgin IV. 2003. Murine cytomegalovirus paralyzes macrophages by blocking IFN gamma-induced promoter assembly. *Proc. Natl. Acad. Sci. USA* 100: 14309–14314.
56. Waller, E. K. 2006. Dendritic cells get VIP treatment. *Blood* 107: 3423–3424.
57. Gonzalez-Rey, E., and M. Delgado. 2007. Vasoactive intestinal peptide and regulatory T-cell induction: a new mechanism and therapeutic potential for immune homeostasis. *Trends Mol. Med.* 13: 241–251.
58. Li, J. M., and E. K. Waller. 2007. The yin and yang of adaptive immunity in allogeneic hematopoietic cell transplantation: donor antigen-presenting cells can either augment or inhibit donor T cell alloreactivity. *Adv. Exp. Med. Biol.* 590: 69–87.
59. Mintern, J. D., E. J. Klemm, M. Wagner, M. E. Paquet, M. D. Napier, Y. M. Kim, U. H. Koszinowski, and H. L. Ploegh. 2006. Viral interference with B7-1 co-stimulation: a new role for murine cytomegalovirus Fc receptor-1. *J. Immunol.* 177: 8422–8431.
60. Sharpe, A. H., E. J. Wherry, R. Ahmed, and G. J. Freeman. 2007. The function of programmed cell death 1 and its ligands in regulating autoimmunity and infection. *Nat. Immunol.* 8: 239–245.
61. Petrovas, C., J. P. Casazza, J. M. Brenchley, D. A. Price, E. Gostick, W. C. Adams, M. L. Precopio, T. Schacker, M. Roederer, D. C. Douek, and R. A. Koup. 2006. PD-1 is a regulator of virus-specific CD8+ T cell survival in HIV infection. *J. Exp. Med.* 203: 2281–2292.
62. Barber, D. L., E. J. Wherry, D. Masopust, B. Zhu, J. P. Allison, A. H. Sharpe, G. J. Freeman, and R. Ahmed. 2006. Restoring function in exhausted CD8 T cells during chronic viral infection. *Nature* 439: 682–687.
63. Kuipers, H., F. Muskens, M. Willart, D. Hijdra, F. B. van Assema, A. J. Coyle, H. C. Hoogsteden, and B. N. Lambrecht. 2006. Contribution of the PD-1 ligands/PD-1 signaling pathway to dendritic cell-mediated CD4+ T cell activation. *Eur. J. Immunol.* 36: 2472–2482.

Supplemental Figure 1

Mice lacking VIP had equivalent numbers of immune cell populations in the blood compared with WT mice. Peripheral blood was collected from naïve VIP-KO and WT mice and stained with fluorescently conjugated monoclonal antibodies to CD45.2, CD3, CD4, CD8, CD11b, B220, TCRαβ, TCRγδ, B220, CD11c, and a lineage cocktail of CD3, DX5, IgM, CD19 and TER119, and analyzed by flow cytometry. Numbers of total leukocytes, or the immune cell subsets shown in the legend, were calculated per μL blood. Open bar represents VIP-KO mice (n=18), Filled bar represents WT mice (n=18). Data are pooled results of 3 replicate experiments.

Supplemental Figure 2

Mice lacking VIP had Th1/Tc1 immune polarization following mCMV infection. VIP-KO and WT mice were infected (day 0) with 5 × 104 PFU mCMV. Splenocytes were collected at baseline prior to infection and 3, 10, and 17 days post-infection, cultured with PMA plus ionomycin and Golgistop for 6 hrs, and then stained with fluorescently conjugated monoclonal antibodies to CD45.2, CD3, CD4, CD8, NK1.1, IFN-γ and TNF-α, and analyzed by flow cytometry. Numbers (per μL of blood) of IFN-γ+ T-cells (A-D), TNF-α+ T-cells (E-H), NK cells (A, E), NKT-cells (B, F), CD4+ T-cells (C, G) and CD8+ T-cells (D, H) following low-dose mCMV infection are shown. * Signifies $p<0.05$, ** signifies $p<0.01$, and *** signifies $p<0.001$, denoting a significant difference between VIP-KO and WT mice. Data pooled from 3 replicate experiments; 12-16 mice were studied at each time-point.

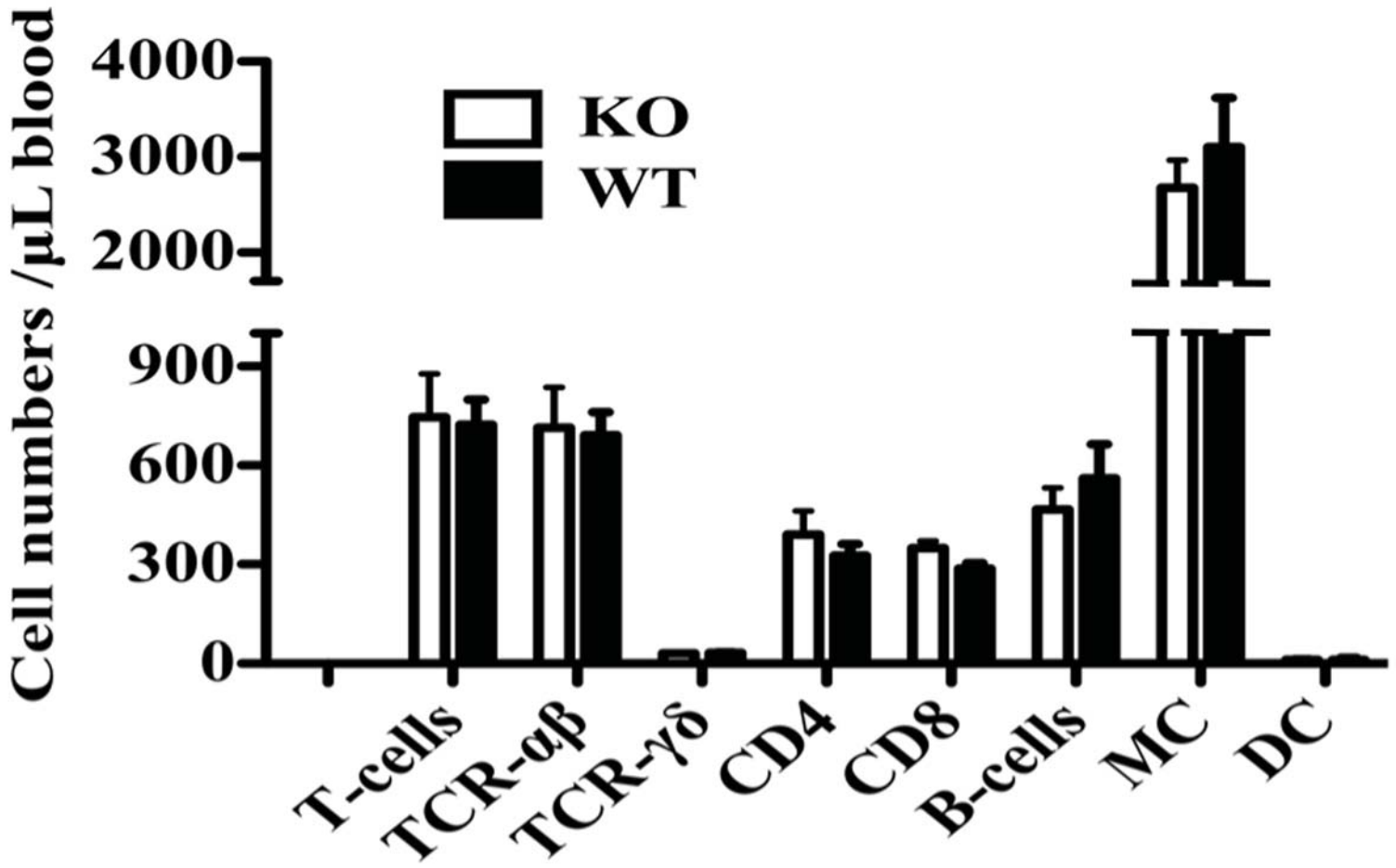
Cell numbers /µL blood
4000
3000
2000
900
600
300
0
KO
WT
T-cells
TCR-αβ
TCR-γδ
CD4
CD8
B-cells
MC
DC

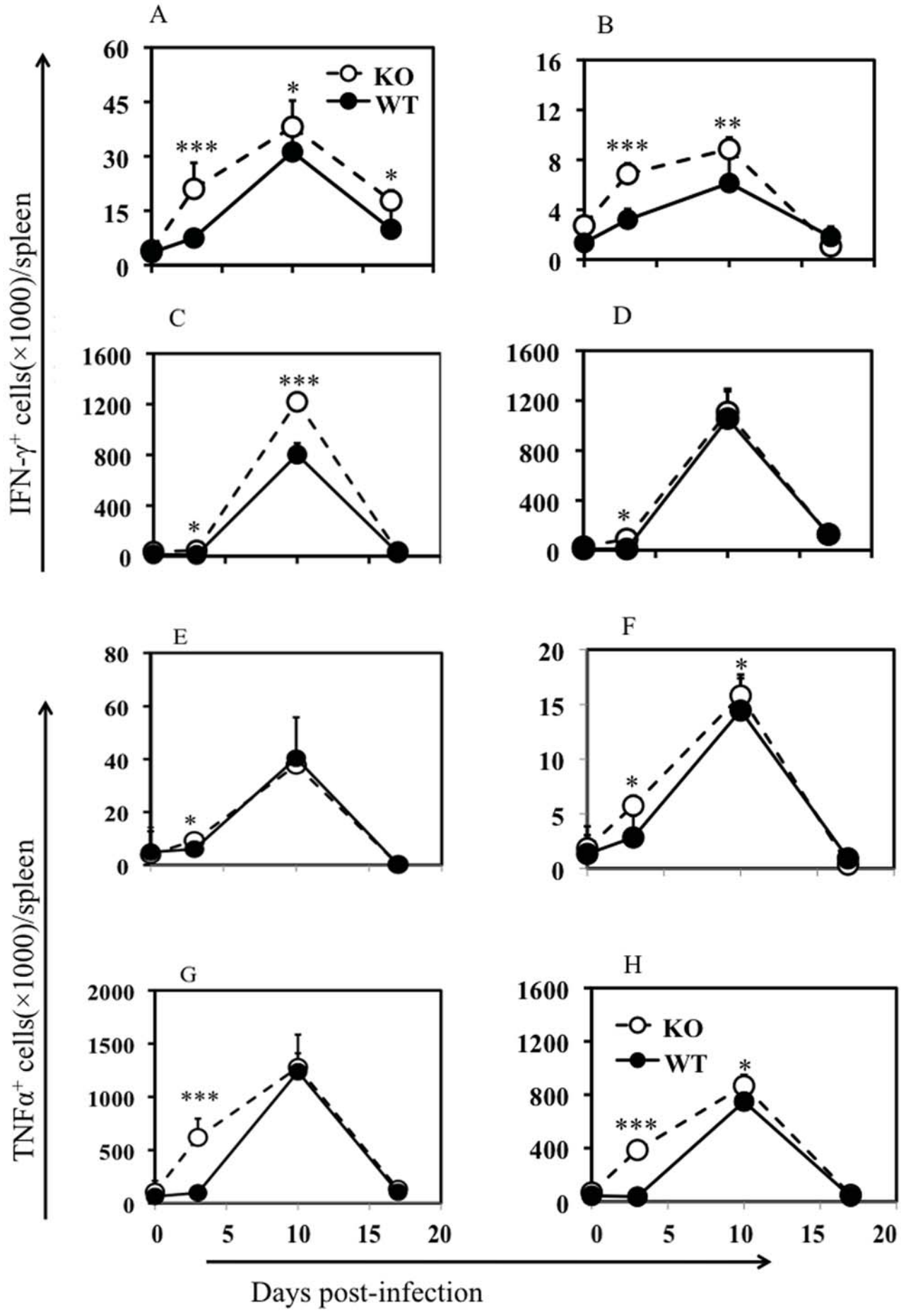
A
B
C
D
E
F
G
H
KO
WT
IFN-γ+ cells(×1000)/spleen
TNFα+ cells(×1000)/spleen
Days post-infection
0
5
10
15
20
60
45
30
15
16
12
8
4
1600
1200
800
400
80
40
2000
1500
1000
500
*
**
***